1 Sun characteristics

Surface temp 5500K, Radius 7e5km, total luminosity 4e33 erg s^{-1}.

2 Basic star properties

More massive stars have increasingly shorter lifetimes. Stars are governed by hydrostatic and thermal equilibrium and live while maintaining a balance between energy generation through nuclear fusion and energy loss through radiation. The lifetime depends on the fusion rate, which scales with temperature to different powers depending on the dominant fuel production.

Sub-photosphere is below the visible surface, where temperature rapidly increases inwards and energy is transported by radiation and convection. Photosphere is where absorption lines are formed. is from about 100km under the surface to 600km outward. This is thus where photons last scatter. Chromosphere has non-thermal heating mechanisms such as magnetic fields, where temperature increases with height. Corona is extremely hot and has low density. Heated by magnetic reconnection and plasma processes. Temperature thus does not monotonically decrease outward.

3 Stellar evolution

Requires nuclear production rates, opacity of stellar plama and an appropriate equation of state. All dependent on density, temperature and composition (mass fraction) X_i

Usually the ideal gas approximation is used assuming non-interacting particles -¿ follow maxwell boltzmann statistics.

When interactions become important you get quantum effects (electron degeneracy pressure, white dwards, red giant cores, neutron stars), radiation pressure (massive stars), magnetic pressure(stellar atmospheres, coronae, accretion disks) and relativistic effects (compact objects: neutron stars, black holes).

Stellar luminosity varies a lot but with little effect on the internal conditions of burning zones, as they self regulate. If fusion increases → pressure increases → core expands → temperature drops → fusion slows If fusion decreases → core contracts → temperature rises → fusion increases

Different densities and temperatures mean different dominant regimes for energy production, which change with evolutionary tracks:

4 Spectra

Spectroscopy done with radiative transfer models. Continuum is made by blackbody spectrums, governed by the Planck function:

$$B_\lambda(T) = \frac{2hc^2}{\lambda^5} \frac{1}{e^{hc/\lambda kT} - 1}$$

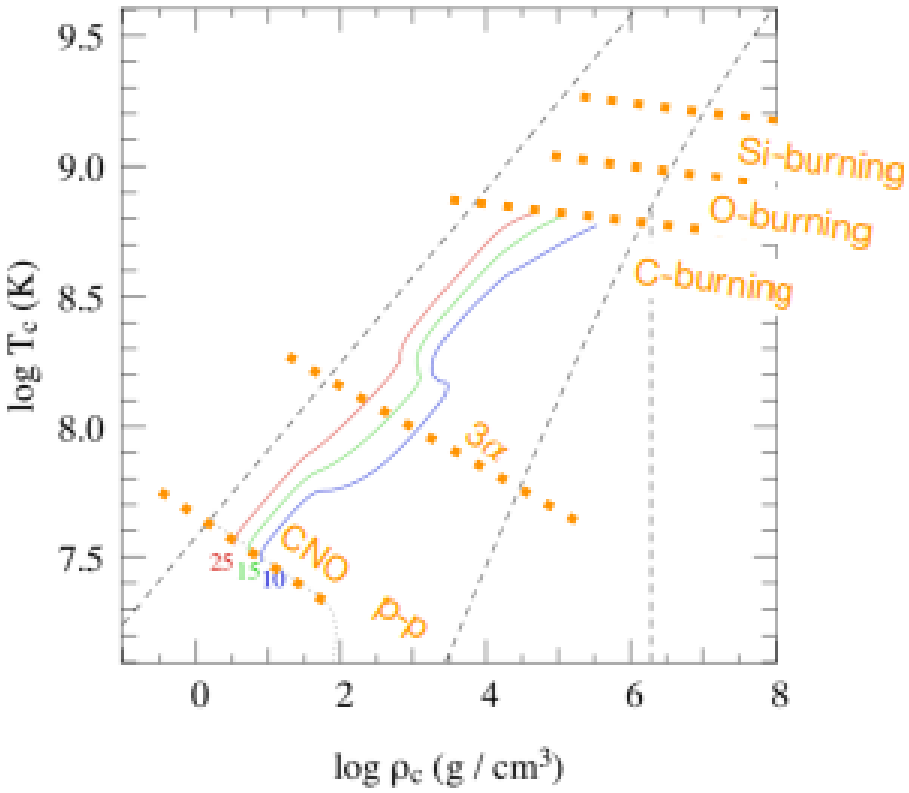

Figure 1: The lines show the evolutionary tracks and how density and temperature change over a lifetime. It shows which burning regimes are significant at which temperature and density boundaries.

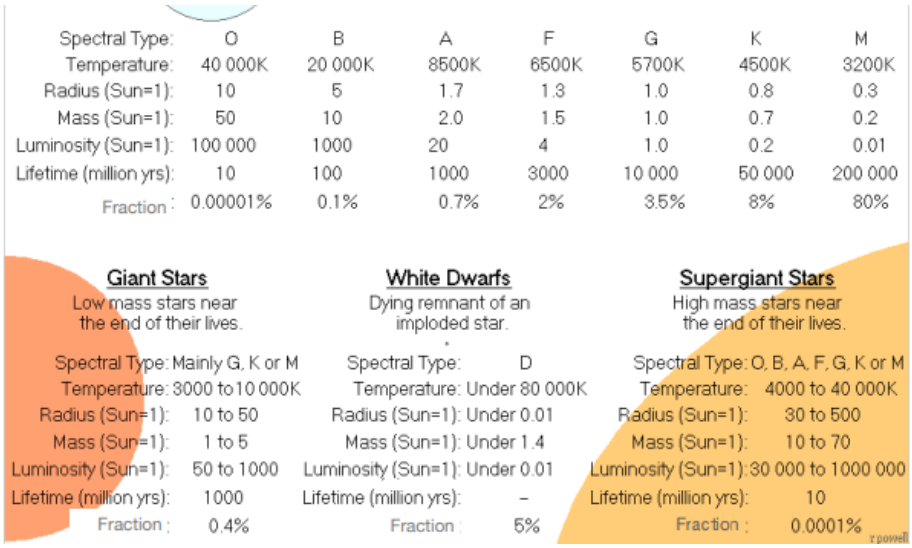

Figure 2: The universe is dominated by low-mass stars, but chemically enriched by massive stars

Luminosity $L_* = 4\pi R_*^2 \sigma T_{eff}^4$ T_{eff} is the black body temperature with the same power output of a star.

Flux at distance r from star $F(r) = \sigma T_{eff}^4 (\frac{R_*}{r})^2$

Magnitude $m_1 - m_2 = 2.5 \log(\frac{F_2}{F_1})$ $m - M \equiv 5 \log(\frac{d}{10pc})$

Lines come from transitions between discrete energy levels. $\lambda = hc/\Delta E_{mn}$ $E_n = -\frac{m_e e^4 Z^2}{2\hbar^2 n^2}$ For hydrogen this becomes:

$$E_n = -\frac{13.6\, eV}{n^2}$$

In order from 1-5 for n_1: Lyman, Balmer, Paschen, Brackett, Pfund.

Excitation of gas governed by Boltzmann equation

$$\frac{n_i}{n} = \frac{g_i e^{-E_i/kT}}{Z(T)}$$

$$Z(T) = \sum_i g_i e^{-E_i/kT}$$

The partition function describes how particles distribute among available energy levels at temperature T

Ionization is governed by the Saha equation.

$$\frac{n_{i+1}}{n_i} = \frac{2}{n_e} \left(\frac{2\pi m_e kT}{h^2} \right)^{3/2} \frac{g_{i+1}}{g_i} e^{-\chi_i/kT}$$

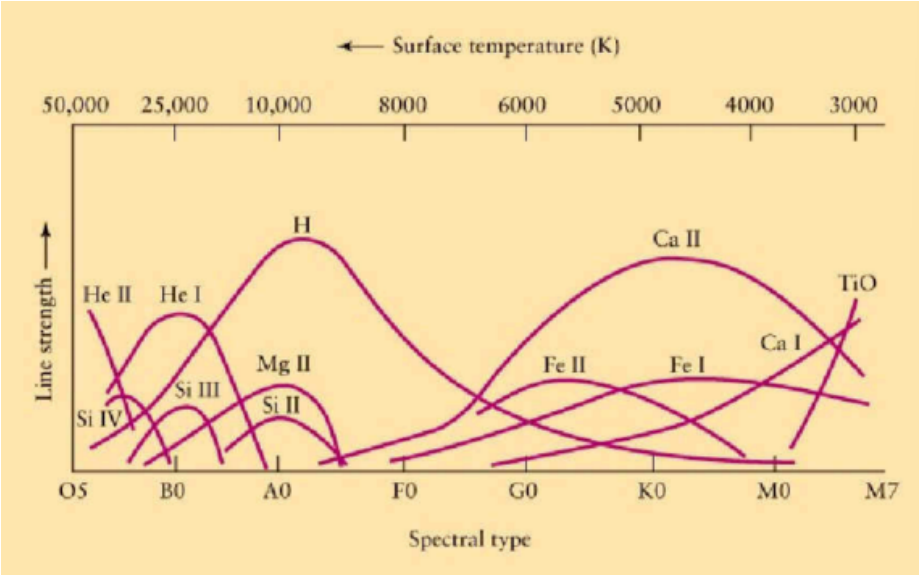

Together this results in dominant features at different temperatures:

Stellar models approximate local thermal equilibrium at certain radii. Non-LTE occurs when radiation dominates over collisions in determining excitation or ionization, which occurs at low density, non-planck radiation field or with really strong lines.

5 Radiative transfer equation

The mean free path is the average distance between photon interactions, given by $\ell = \frac{1}{\kappa_\nu \rho}$. On a macroscopic level this defines the cumulative optical thickness along a path $\tau = \int \frac{1}{\ell} ds$, where $\tau = 1$ means photons have about a $\frac{1}{e} \approx 37\%$ chance of survival without interacting.

The overall interactions are described by the radiative transfer equation $\frac{dI_\nu}{dz} = -k_\nu \rho I_\nu + j_\nu$, which thus depends on physical depth z. Density and opacity can vary strongly with small changes in z making this quite hard to actually solve, thus optical depth is more commonly used. κ_ν is opacity, ρ density, j_ν emissivity.

5.1 Eddingtons Radiative Equilibrium model

Assumes a plane parallel atmosphere, LTE, radiative equilibrium (no convection), isotropic radiation, frequency independent opacity, no scattering and hydrostatic equilibrium. Thus we get energy conservation meaning flux is constant with geometric depth.

Radiation originates from various optical depths. Even though temperature increases inwards, most of the contribution to intensity comes from around $\tau = 1$. Further inwards more gets absorbed.

- bound-bound: electron transitions between bound states, leading to spectral lines.
- bound-free: Electron absorbs photon and escapes atom, leading to continuum absorption edges
- free-free: free electron accelerated in ion field, leads to smooth continuum

5.2 Rosseland mean opacity

$$\frac{1}{\kappa_R} = \frac{\int_0^\infty \frac{1}{\kappa_\nu} \frac{\partial B_\nu}{\partial T} \, d\nu}{\int_0^\infty \frac{\partial B_\nu}{\partial T} \, d\nu}$$

Rosseland mean weights transparent frequencies more strongly. It is a transport-weighted opacity, not emission-weighted.

6 Model photosphere

A phase parallel geometry is often used to model the photosphere, where we take a column with height x and model along that, but often we want to use optical depth $\tau_\nu = \int_0^L \kappa_\nu \rho dx$. We then use that to derive a hhydrostatic equation, which we can solve to get $P_g(\tau_0)$, but then we need to know κ_0 as a function of τ_0, which depends on temperature and electron pressure. Thus we need to follow the following steps to get a stellar photosphere model:

1. Establish T(τ_0) through i.e. Eddington gray atmosphere
2. Establish Pe(τ_0), depending on Saha, composition, metallicity
3. Make a first guess for Pg(τ_0) through hydrostatics with approximated opacity
4. Numerically integrate and improve on Pg(τ_0)
5. Repeat steps 3. and 4. until convergence

We start with the temperature through limb darkening, where the stellar disk appears darker at the edge because you dont see deeper layers, or possibly through strong line formation. For the pressure we have to look at metallicity, as higher metallicity means more free electrons, which leads to larger continuus absorption coefficient, thus a shorter geometric line of sight, and thus a lower gas pressure. The most important metals are C, Si, Fe, Mg, Ni, Cr, Ca, Na, K.

7 Spectral Lines

Spectral lines give info on line-of-sight velocity, temperature, surface gravity, chemical composition, rotation and photosphere structure, but disentangling these effects is hard. Line shapes are not perfect delta functions, due to natural broadening, pressure broadening (collisions and microturbulence) and doppler (thermal) broadening. These give gaussian effects, the resulting profile is a Voigt function. Line strength is determined by the ratio of line absorption to continuous absorption.

Microturbulence shape cannot really be measured, so its assumed Gaussian and isotropic. Micro is when length scale of velocity field is less than photon mean free path, this affects line width and depth. Macroturbulence is the opposite and affects line shape. Only the former affects equivalent width.

Equivalent width is often used to measure line properties, which is when a rectangular line from 0 to I intensity has the same area as the spectral line profile area.

Curve of growth relates equivalent width to abundance When the curve of growth is weak, the equivalent width of lines is nearly proportional to the abundance, and the gaussian shape dominates. The core saturates when the curve does, and with strong lines the wings dominate the shape.

Pressure affects only some lines, others are unaltered. Damping wings are pressure sensitive, and the linear stark effect (broadening due to electric fields in plasma) is pressure sensitive. So lines get broader for high g and high P, so lines broaden more in dwarfs than giants, and least in supergiants.

A spectrograph can be used to measure spectral lines. A diffraction grating is used to measure transmission, assuming the incoming wave is planar. A spectrograph has a certain resolving power dependent on slit spacing and slit width. Echelle spectrograph uses coarse grating and higher order diffraction to achieve very high resolving power over a wide wavelength range.

For computing and measuring spectral lines, we can use models like pySME which use linelists, such as 4MOST, which are based on precomputed energy transitions. log(gf) is also a factor where g is a statistical weight and f the oscillator strength, which together measures the intrinsic line strength. log(gf) can be measured empirically from branching fractions and lifetimes, but they can also be computed theoretically. Different linelists have slightly different parameters and can impact abundance analysis.

8 Nucleosynthesis

Metallicity affects the track followed in the HR-diagram. 4 types of nucleosynthesis: big bang, stellar, explosive and cosmic ray spallation.

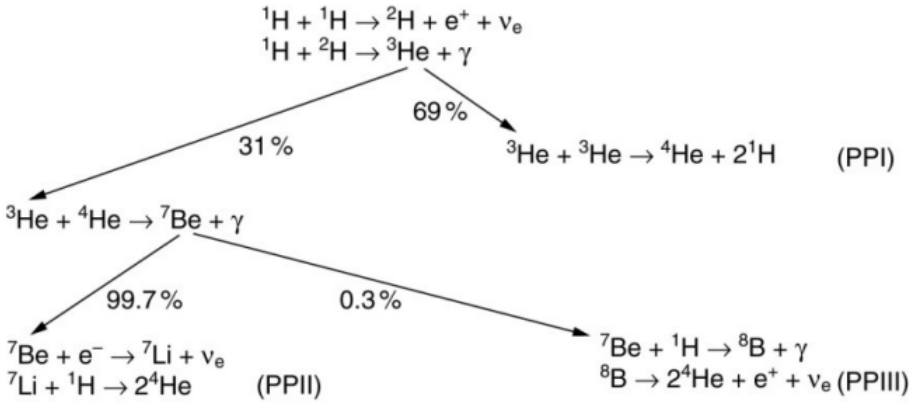

Figure 3: Fractions are valid for the sun, neutrinos carry away energy and positrons produce energy through annihilation

8.1 Stellar nucleosynthesis

Hydrogen burning -¿ He, C, N, O, F, Ne, Na Helium burning -¿ C+ 16O, 20Ne, 24Mg alpha-process -¿ adding 4He to 20Ne to form 24Mg, 28Si, 32S, 36A, 40Ca. equilibrium process: Very high temp and dens make iron group: V, Cr, Mn, Fe, Co, Ni s-process: abundance peaks at A=90,138,208 r-process: Heaviest elements U, Th. Peaks at A=80,130, 194 p-process: Very low abundances of p-rich isotopes.

8.2 Main Sequence Burning

The dominant process for H fusion in the main sequence depends on mass. For below 0.08 solar mass most dominant is 7Li+1H = 4He+4He or 2H + 1H = 3He + γ Above 1.5 solar mass the proton-proton chains and CNO cycles are most important.

9 Evolution of Low Mass stars

The evolution is commonly shown in a Kippenhahn diagram:

Main Sequence: Core H-burning (p-p chain, radiative core, convective envelope. Subgiant branch: Core H exhausted, H-burning moves to shell, core contracts, envelope expands Red Giant Branch: Inert He core, H-burning shell, large convective envelope, star becomes luminous and cool Helium Flash (for very low mass): Degenerate He core, explosive He ignition, no surface explosion, energy absorbed internally Horizontal branch: Stable core He-burning, H-burning in shell continues Asymptotic Giant Branch: Inert C-O core, He-burning shell + H-burning shell, large convective envelope.

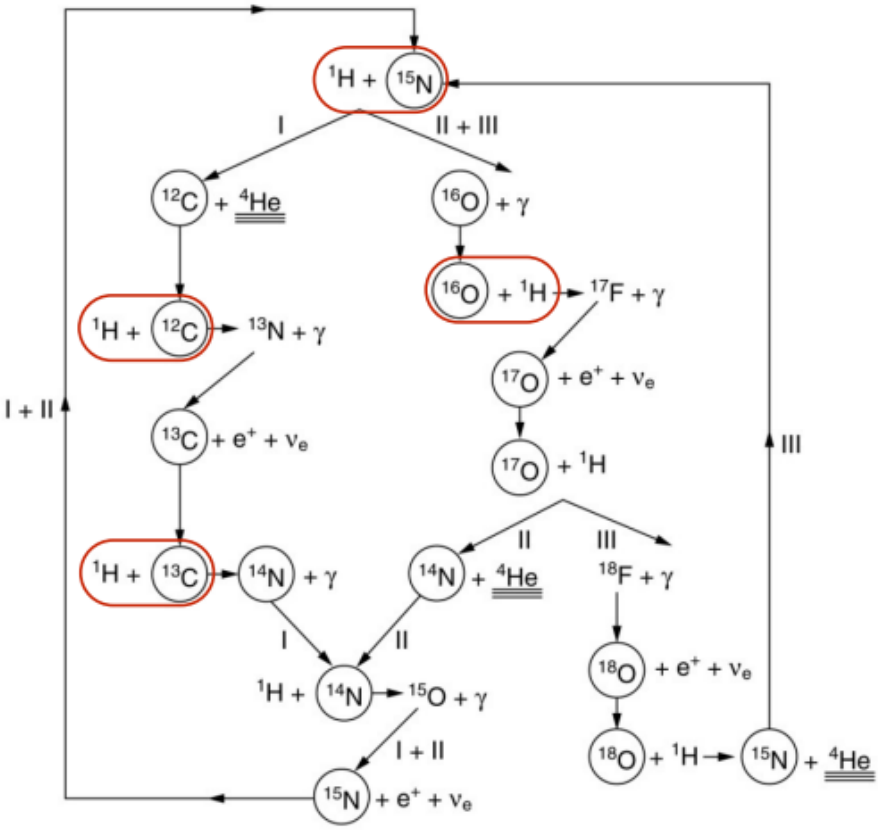

Figure 4: Netto reaction: 4 ^{1}H $\rightarrow^{4}$He + 2e^{+} + 2ν_e + 3γ. Dominates above 1.5 solar mass, but also contributes at lower mass.

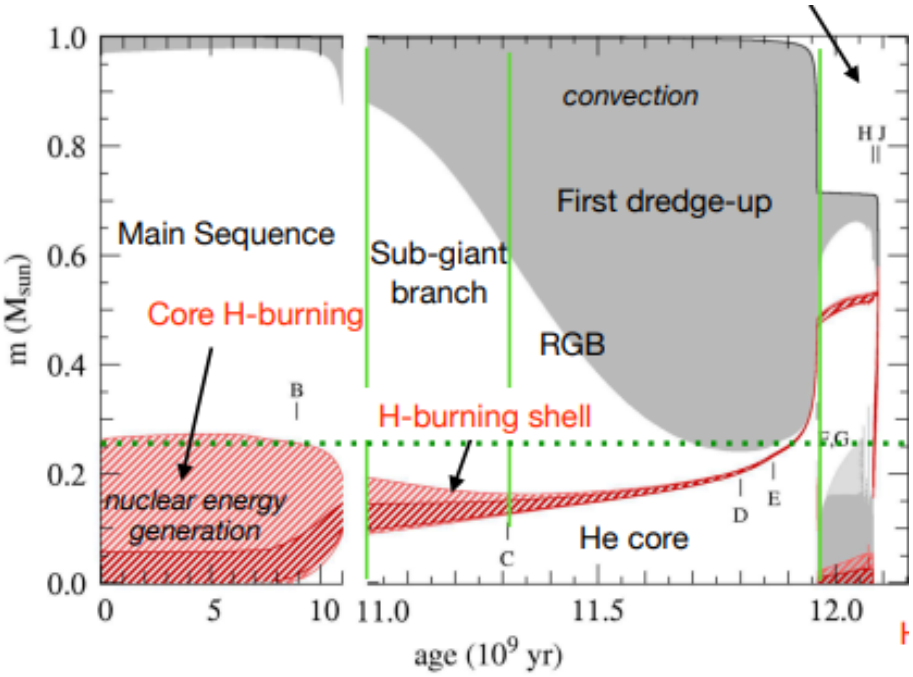

Figure 5: Shows the internal structure of a star over time. Bottom is core, top is surface. Dark shaded regions are convective zones, light is radiative zones.

Nuclear fuel	*Process*	$T_{\text{threshold}}$ $(10^6\ K)$	*Products*	*Energy per nucleon (MeV)*
H	$p-p$	~4	He	6.55
H	CNO	15	He	6.25
He	3α	100	C, O	0.61
C	C + C	600	O, Ne, Na, Mg	0.54
O	O + O	1000	Mg, S, P, Si	~0.3
Si	Nuc. eq.	3000	Co, Fe, Ni	<0.18

A dredge-up is the deepening of the convective envelope into nuclear-processed layers, bringing fusion products to the surface. First dredge-up: Red giant branch, convection reaches H-burning products, Surface He goes up, 14N up, 12C down, 12C/12C ratio down. Second dredge-up: Intermediate mass stars, after core He burning, brings He and CNO products to surface Third dredge-up: AGB, after thermal pulses, brings 12C, s-process elements and heavy nuclei to surface. Signatures of dredge ups in surface abundance over time plots are sudden jumps in C,N-Na, s-process elems. Each jump is a dredge-up event.

Na-Ne cycle: Part of advanced H-burning at high temps, converting 22Ne to 23Na. Signature = sodium enrichment at surface after dredge-up. Mg-Al cycle: At high temp H-burning, 24Mg+25Al to 25Mg, Signature=Mg depletion and Al enhancement. Seen in globular clusters and AGB-processed material

10 Evolution of intermediate mass stars

At higher mass we get core Helium burning. At this moment the shell still can burn H. Helium burning produces carbon, 16O, 20Ne and maybe 24Mg.

Intermediate mass stars go through an AGB phase, which results in a second and maybe a third dredge up, increasing He, 14N, 23Na at the surface but reducing 12C and 16O. Thermal pulses occur, which are periodic helium shell flashes caused by unstable He burning. Occurs when He-shell accumulates fuel, temp rises, He burning ignites explosively, energy release expands layers, burning shiuts off, cycle repeats. Leads to flash driven convection as He flash creates convective zone in He burning shell. This mixes C and s-process elements which enable neutron sources, powering the s-process.

In AGB stars we see evidence for the s-process, which occurs in He-burning shells.

Stellar mass vs. Nuclear burning phases

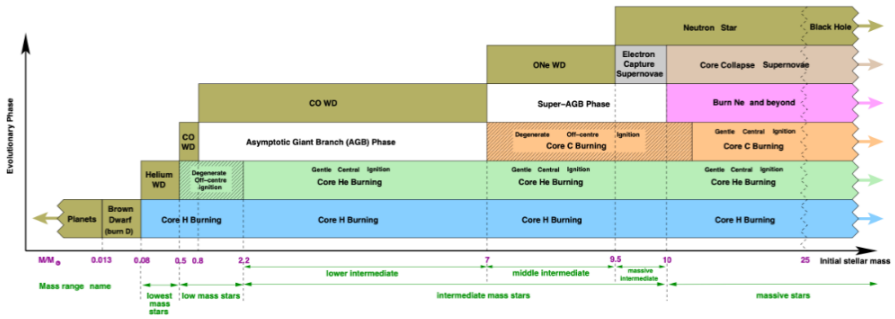

11 Type 1A supernovae

White dwarfs have similar mass but a lot smaller radius, thus higher density, than solar type stars. Electrons are forced into higher momentum states at low temperatures due to Pauli exclusion principle = Degeneracy pressure. Type 1A supernovae produce Ni, Fe, Co, Cr, Mn primarily. Per event they create about half a solar mass of iron, it is the dominant source of iron production. Progenitors can be 2 scenarios: double and single degenerate, depending if its white dwarf + regular star or 2 white dwarfs. Extra mass inflow pushes white dwarf over Chandrasekar mass, the limit above which electron degeneracy pressure is insufficient to balance star gravity. Different subclasses such as sub chandrasekar mass SN1a (He layer accretes onto white dwarf, detonates, shock compresses core) can produce different mixtures of chemical elements and differ in delay times.

12 Type 2 (core collapse) supernovae

Responsible for half the elements of the periodic table, but not fully understood. Six majors fuels principle burning stages in massive stars: H-CNO, p-p chain, 4He-3α producing 12C, 12C-12C to 16O, where fate of the star is determined by 12C/16O ratio and CO core mass? Then consecutive phases with faster contraction: 12C -¿ 20Ne -¿ 16O -¿ 28Si -¿ iron peak. Each phase is thus shorter and shorter.

The biggest source of uncertainty in models is convection. The initial mass of the star is less important than the mass right before exploding. Magnetic fields and energy generation in different layers is poorly understood and has large uncertainties. Also, most massive stars are in binary systems while models assume singular.

Phases of SNII: collapse phase when core is iron, shutting off nuclear reaction, making gravity dominant. Density increases rapidly and neutrinos get trapped. When nuclear saturation is reached, collapse stops and a pressure wave turning shock wave travels outwards. The bounce phase is when the shock photo-dissociatiates and loses energy due to photodisintegration of iron. It can recede or be re-energized. Neutrino delayed heating is when neutrino heating keeps the shock going together with either neutrino-driven turbulent convection or the standing shock instability (large scale oscillations of the stalled shock). If the shock is re-energized, all material is pushed away leaving behind a neutron star from the innermost layers. Else, core collapses and black hole forms.

SNII are sources of neutron-deficient isotopes such as 84Sr, 132Ba, 138La, 144Sm, 152Gd, which cannot be synthesized by neutron capture processes.

i-process occurs between s and r, in some AGB and post AGB stars and flash-driven convection zones. Signature = Mixed abundance patterns not explained by s or r alone.

Cosmic Ray spallation is responsible for the abundance of some light elements such as lithium, beryllium and boron.

13 Galactic Archaeology

Important is to measure stars position, distance, radial velocity and tangential velocity, creating a 6D phase space. Distances are often obtained by comparing to known sources/standard candles. Distances can be obtained from (a combination of) parallax, colours and priors on the milky way distribution. Radial velocity is measured using spectral line shifts (doppler). Tangential velocity through Gaia proper motion + distance.

Earliest stars with [Fe/H] have very low metallicity of like -5, but there are about 40 stars known compared to the millions of solar metallicity stars.

Isochrones are curves in the HR diagram representing stars of the same age but different masses and evolutionary stages. They can be used as metallicity-sensitive tools. They can also be used to measure ages of stars, less accuracy for older stars and red giant branch. Uses stars with known age range such as cepheids (Pulsating stars with a tight period–luminosity relation) and uses chemical abundances.

Earliest stars would be ultra metal poor, with unusual abundance patterns. But very difficult to find. They are targeted by i.e. the Pristine survey and Gaia XP spectra with a very narrow band. Extremely metal poor stars can be mistaking classified as hot or noisy. Also if there are no lines to fit its hard to find a spectroscopic solution.

13.1 Astroseismology

Oscillations in stars can be used for age determination. Different modes (pressure modes, gravity modes and mixed modes) probe different depths of the star.

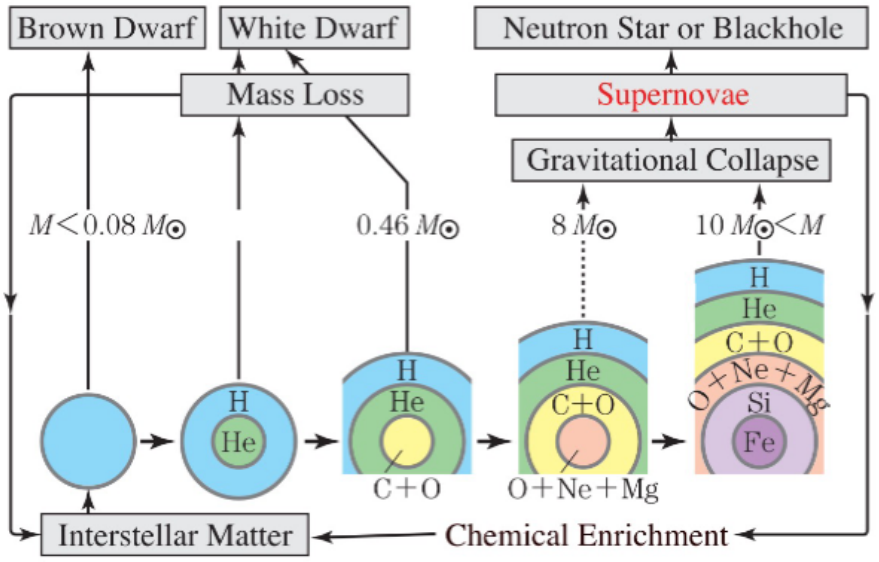

Figure 6: The fate of stars depending on their initial mass M (single stars only). Threshold depends om metallicity

Sound speed changes can be mapped, such as between convective and radiative layers. Thats how we know the sun rotates slower in the inner parts.

14 Stellar populations and Dwarf galaxies

Stellar abundances and kinematics are excellent tools for galactic archaeology to disentangle the milky way. Enrichment tells us about star formation history but is difficult to accurately determine. It requires a high spectral resolution and also it is more difficult for lower metallicity. In Metallicity Distribution Functions ([α/Fe] vs [Fe/H] plots) we see rapid enrichment of α elements through core collape SN, delayed enrichment from SNIa for Fe. The knee in this diagram signifies the onset of SNIa. This knee moves to lower [Fe/H] from bulge-¿disk-¿dwarf galaxies (left with lower star formation). Note that high mass stars enrich much faster and low mass stars can have a very very long lifetime.

Quasar spectra of high redshift can have absorption lines that are often exclusively from intervening gas, sometimes intergalactic medium and sometimes galaxies. IGM is important for replenishing star formation fuel when absorbed into galaxies.

15 Modeling chemical evolution

Step 1: Define gas fraction and metallicity

$$f_g = \frac{M_{\rm gas}}{M_{\rm tot}}, \quad Z = \frac{M_{\rm metals}}{M_{\rm gas}}$$

Step 2: Stellar yield

$$dM_{\rm metals} = y\, dM_*$$

Step 3: Metals in gas

$$M_Z = Z M_{\rm gas} = Z f_g M$$

Step 4: Differential equation for metal mass

$$d(M_Z) = d(Z f_g M) = M(Z\, df_g + f_g\, dZ) = -yM\, df_g$$

Step 5: Simplify

$$Z\, df_g + f_g\, dZ = -y\, df_g \quad \Rightarrow \quad f_g\, dZ = -(y+Z)\, df_g$$

Step 6: Separate variables

$$\frac{dZ}{y+Z} = -\frac{df_g}{f_g}$$

Step 7: Integrate

$$\int_0^Z \frac{dZ'}{y+Z'} = -\int_1^{f_g} \frac{df_g'}{f_g'} \quad \Rightarrow \quad \ln\frac{y+Z}{y} = -\ln f_g$$

Step 8: Solve for Z

$$\frac{y+Z}{y} = \frac{1}{f_g} \quad \Rightarrow \quad Z = y\left(\frac{1}{f_g} - 1\right) = y\frac{1-f_g}{f_g}$$

Some assumptions made that are inaccurate:

1. The system is isolated, thus mass is conserved. Breaks in galaxies with inflow/outflow and dwarfs
2. The gas in the system is well-mixed. Breaks in turbulent disks and mergers
3. Initially the system consists of pristine gas with no metals. Breaks at later gelaxies/merger remnants
4. Stars immediately return their metals to the gas, breaks for low mass and SNIa.

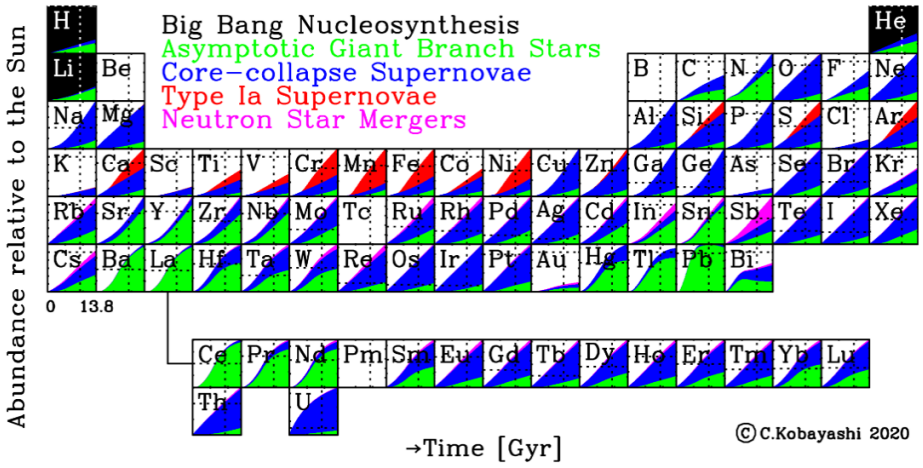

Full chemical evolution is a more complex, requires integrating:

$$\frac{d(Z_i f_g)}{dt} = E_{SW} + E_{SN_{cc}} + E_{SNIa} + E_{NSM} - Z_i\psi + Z_{i,inflow}R_{inflow} - Z_i R_{outflow}$$

ψ is star formation rate, E_{SW} is stellar winds. Assumes gas is immediately well mixed. First 2 terms are only nucleosynthesis, 3rd and 4th are also modelling of progenitor binaries, last 3 are galactic.

Nucleosynthesis yields and enrichment is dependent on metallicity and must be determined on the fly, the yields have to then be integrated over stellar lifetimes. At extremely low mass stars this yield is unclear, but these stars have lifetimes of longer than the age of the universe so that is not an issue.

$$E_{SNIa} = m_{CO} p_{Z_i m,Ia} \mathcal{R}_{t,Ia}$$

$\mathcal{R}$ is the rate of supernovae per unit time per unit stellar mass. m_{CO} is all the matter in the white dwarf that is ejected from SNIa. E_{NSM} dependent on rate and the fraction ejected, similar to SNIa.

Star formation rate is sometimes unclear, often proportional to the gas fraction. Inflow rate is often assumed exponential. For cosmological inflow, primordial composition thus no metals is assumed. Outflow rate is often proportional to the star formation rate, but can be separate for example for quenched galaxies. For satellite dwarf galaxies, mass loss due to tidal or ram-pressure stripping may also be important.

Both in observations and simulations, more massive galaxies tend to have higher metallicities, which is called mass–metallicity relations (MZR). Bulge has high α/Fe at high Fe/H. Signifies rapid SF, SNII dominates. Thin disk has lower α/Fe and gradual decrease. Signifies lower SF, SNIa contribute over longer times. Thick disk has high α/Fe plateau, signifying old stars and fast SF

early on. Dwarf galaxies have knee t low [Fe/H] and have low [α/Fe], signifying slow SF and delayed contribution of SNIa

Milky way shows opposing evidences between thick and thin disk, possibly caused by a two-infall model or formation of thick disk stars in sattelite galaxies.